Title
Radial Diffusion and Penetration of Gas Molecules and Aerosol Particles through Laminar Flow Reactors, Denuders, and Sampling Tubes

Journal
Analytical Chemistry, 87(7)

ISSN
0003-2700

Authors
Knopf, Daniel A
Pöschl, Ulrich
Shiraiwa, Manabu

Publication Date
2015-04-07

DOI
10.1021/ac5042395

Peer reviewed

analytical chemistry

Article

pubs.acs.org/ac

Radial Diffusion and Penetration of Gas Molecules and Aerosol Particles through Laminar Flow Reactors, Denuders, and Sampling Tubes

Daniel A. Knopf,*[,†] Ulrich Pöschl,[‡] and Manabu Shiraiwa*[,‡]

[†]Institute for Terrestrial and Planetary Atmospheres, School of Marine and Atmospheric Sciences, Stony Brook University, Stony Brook, New York 11794, United States

[‡]Multiphase Chemistry Department, Max Planck Institute for Chemistry, 55128 Mainz, Germany

ABSTRACT: Flow reactors, denuders, and sampling tubes are essential tools for many applications in analytical and physical chemistry and engineering. We derive a new method for determining radial diffusion effects and the penetration or transmission of gas molecules and aerosol particles through cylindrical tubes under laminar flow conditions using explicit analytical equations. In contrast to the traditional Brown method [Brown, R. L. *J. Res. Natl. Bur. Stand. (U. S.)* **1978**, *83*, 1−8] and CKD method (Cooney, D. O.; Kim, S. S.; Davis, E. J. *Chem. Eng. Sci.* **1974**, *29*, 1731−1738), the new approximation developed in this study (known as the KPS method) does not require interpolation or numerical techniques. The KPS method agrees well with the CKD method under all experimental conditions and also with the Brown method at low Sherwood numbers. At high Sherwood numbers corresponding to high uptake on the wall, flow entry effects become relevant and are considered in the KPS and CKD methods but not in the Brown method. The practical applicability of the KPS method is demonstrated by analysis of measurement data from experimental studies of rapid OH, intermediate NO_3, and slow O_3 uptake on various organic substrates. The KPS method also allows determination of the penetration of aerosol particles through a tube, using a single equation to cover both the limiting cases of high and low deposition described by Gormley and Kennedy (*Proc. R. Ir. Acad., Sect. A.* **1949**, *52A*, 163−169). We demonstrate that the treatment of gas and particle diffusion converges in the KPS method, thus facilitating prediction of diffusional loss and penetration of gases and particles, analysis of chemical kinetics data, and design of fluid reactors, denuders, and sampling lines.

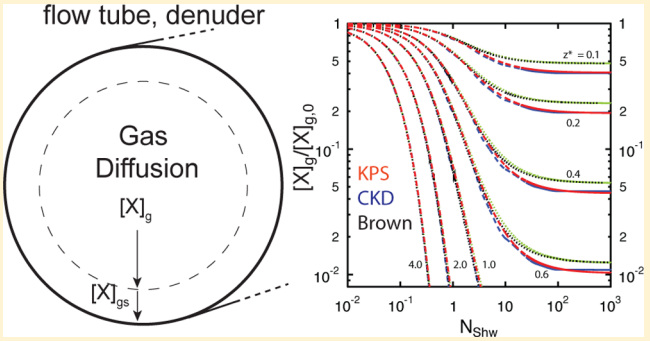

Flow reactors and diffusion denuders are applied in many fields of chemistry and engineering. Flow tubes are used to investigate the chemical kinetics of gas and heterogeneous and multiphase reactions in catalytic, combustion, vapor deposition, environmental, and atmospheric processes, and diffusion denuders are used to separate gases from particulate matter for chemical analysis of aerosols.[1−22] For example, flow tubes are often used to study reactive gas uptake[23−33] and the formation and evolution of atmospheric aerosol particles.[34,35] For accurate analysis and interpretation of flow-tube experiments investigating the products, kinetics, and mechanisms of heterogeneous reactions, it is necessary to understand and quantify the interaction of gases and particles with the reactor walls, which inherently involves mass transport by diffusion to the surface.[36,37] For example, at high pressure and small gas diffusivity, mass transfer can be kinetically limiting and leads to significant underestimation of chemical reactivity and rate coefficients determined by coated-wall flow-tube experiments.[38,39]

Several analytical and numerical methods exist to describe the influence of gas-phase diffusion on gas uptake by an absorbing or reactive surface.[40−42] For spherical surfaces and application to aerosol particles, Fuchs[43] and Fuchs and Sutugin[44] provided analytical solutions to the problem. Following up on their approaches, Pöschl, Rudich, and Ammann (PRA)[45,46] derived and introduced a gas-phase diffusion correction factor that provides a straightforward description and robust quantification of gas-diffusion effects on gas−particle interactions in aerosols, clouds, and related kinetic models.[45−52]

The most commonly applied methods for prediction of penetration and gas-phase diffusion in flow-tube reactors and denuders are the numerical method by Brown[53] and interpolation method by Cooney−Kim−Davis (CKD).[54,55] Brown[53] provides a numerical approach of correcting pseudo-first-order reaction kinetics between gas species and surface implicitly accounting for radial diffusion effects.[56] Murphy and Fahey[55] present a numerical method based on an interpolation

Received: November 12, 2014
Accepted: March 5, 2015
Published: March 5, 2015

DOI: 10.1021/ac5042395
Anal. Chem. 2015, 87, 3746−3754

of the CKD solution to correct for diffusion in gas uptake by the walls of a cylindrical flow tube or denuder. The loss of aerosol particles to the cylindrical wall of a flow reactor or denuder is usually evaluated by applying the analytical solution of Gormley and Kennedy (GK).[14,15,57−62] For highly absorbing walls, the GK solution provides the limit of the CKD solution.[55]

Here, we follow up on the PRA approach to derive, in combination with the previously determined diffusion-limited uptake,[40,63−65] the penetration or tube transmission and the radial diffusion correction factor, $C_{g,X}$, for gas uptake or loss to absorbing or reactive wall surfaces in cylindrical laminar flow reactors and denuders. In contrast to previous treatments of this problem, where the absorbing or reactive wall surface was taken as a boundary condition, we follow the flux matching approach of Fuchs and Sutugin[44] and Pöschl et al.,[46] where the fluxes of gas-phase diffusion and net uptake are matched at about one mean free path above the absorbing or reactive wall surface. The new method derived in this study (Knopf−Pöschl−Shiraiwa, KPS) enables efficient and robust analyses and predictions of gas and particle uptake and penetration in flow-tube experiments as well as the design and application of diffusion denuders and sampling tubes by use of explicit analytical equations. Our approximation circumvents the need for numerical and interpolation methods. We perform and present a systematic comparison and validation of the results of the KPS method against the Brown numerical method and the CKD interpolation method covering a wide range of flow conditions and surface uptake. Furthermore, we demonstrate the practical applicability of the KPS method by analysis of measurement data from three experimental flow-tube studies that involve reaction of gaseous OH, NO_3, and O_3 with a variety of organic surfaces, spanning a broad range of flow-tube operation conditions and surface reactivity. Finally, we show that the KPS method can also be applied to describe particle losses to the wall of a tube and validate the results against the established solutions of Gormley and Kennedy.[61]

CONCEPT AND EQUATIONS

In flow-tube and denuder experiments, it is common practice to record the gas-phase concentration of the investigated species relative to its initial concentration, $[X]_g/[X]_{g,0}$, frequently called penetration or tube transmission,[14,15] and to describe the concentration change along the tube by pseudo-first-order reaction kinetics.[1,3,53,56] Under laminar flow conditions, the gas species X will travel faster in the flow-tube center than close to the wall, resulting in a radial gradient of concentration that depends on flow velocity, tube geometry, and diffusion. The wall loss or net uptake of a gas species is determined by a sequence of processes including mass transfer from the gas phase to the wall surface and chemical reactions on the surface or in the bulk of the wall material or coating, which may follow the well-known Langmuir−Hinshelwood[66,67] and Eley−Rideal[68,69] reaction mechanisms and kinetics.[46]

A detailed discussion on the gas-phase diffusion correction for spherical particles has been provided by Pöschl et al.[46] We follow their definitions and nomenclature when deriving the gas-phase diffusion correction for the cylindrical geometry of a flow-tube reactor.

Similar to previous studies addressing gas-phase correction for derivation of gas uptake kinetics in flow-tube reactors,[53,55] the following assumptions are made for derivation of the analytical equations: (a) the interacting gas species is a trace gas in the bulk flow, (b) laminar flow is established in the flow reactor, (c) the gas temperature and viscosity are homogeneous, (d) the axial diffusion velocity is negligible compared to bulk flow velocity, (e) the amount of gas species taken up is small compared to its reservoir, and (f) there is an absence of gas-phase reactions impacting gas species concentration. Laminar flow is present in flow tubes when the Reynolds number, Re, is smaller than ∼2000,[70] which is typically the case for flow-tube reactor studies. The Peclet number, Pe_X, describes the ratio of advective transport rate to diffusive transport rate:[70]

$$Pe_X = \frac{D_{tube} v_{g,X}}{D_{g,X}} \tag{1}$$

where $v_{g,X}$ is flow velocity, $D_{g,X}$ is the gas-phase diffusion coefficient of species X, and D_{tube} is tube diameter. For $Pe_X > \approx 10$, axial diffusion can be neglected. The length after which a laminar profile is established in a flow tube can be estimated as[71] $L \approx 0.035 D_{tube} Re$. Usually L is much shorter than the tube length, l_{tube}. The dimensionless axial distance, z^*, is defined by normalizing the axial distance z in the tube ($z \le l_{tube}$) by the ratio of $D_{g,X}$ to volumetric flow rate (Q):[55]

$$z^* = z\left(\frac{\pi}{2}\right)\left(\frac{D_{g,X}}{Q}\right) \tag{2}$$

Kinetics uptake studies determine the uptake coefficient (or wall reaction probability) of gas species X, which can be defined as

$$\gamma_X = \frac{J_{net,X}}{J_{coll,X}} \tag{3}$$

where $J_{net,X}$ and $J_{coll,X}$ represent the net and collision flux of X to the surface, respectively. $J_{coll,X}$ can be expressed as

$$J_{coll,X} = [X]_{gs}\frac{\omega_X}{4} \tag{4}$$

where $[X]_{gs}$ is the concentration of X in the near-surface gas phase, within about one mean free path, λ_X, of the surface[46] (see Figure 1), and ω_X is the thermal molecular velocity of species X. In case of significant uptake, $[X]_{gs}$ is usually smaller than the average concentration of X in the gas phase away from

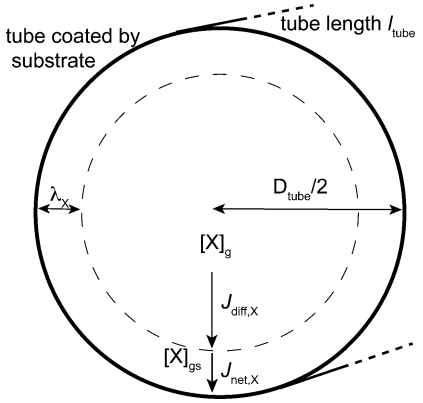

Figure 1. Schematic illustration and key parameters of a cylindrical flow reactor, denuder, or sampling tube: tube diameter, D_{tube}, and tube length, l_{tube}; average gas-phase concentration of species X, $[X]_g$, and its near-surface gas-phase concentration, $[X]_{gs}$, about one mean free path, λ_X, off the absorbing or reactive wall surface; and fluxes of diffusion, $J_{diff,X}$, and net uptake, $J_{net,X}$.

DOI: 10.1021/ac5042395
Anal. Chem. 2015, 87, 3746−3754

the surface, $[X]_g$ (if it is assumed that X is homogeneously distributed). As a consequence, it always holds that

$$J_{coll,X} \leq [X]_g \frac{\omega_X}{4} = J_{coll,avg,X} \quad (5)$$

In experimental studies, $[X]_g$ is an observable, and thus it is useful to define $J_{net,X}$ as

$$J_{net,X} = \gamma_{eff,X} J_{coll,avg,X} = \gamma_{eff,X}[X]_g \frac{\omega_X}{4} = \gamma_X [X]_{gs} \frac{\omega_X}{4} \quad (6)$$

with $\gamma_{eff,X}$ representing the apparent or measurable or effective uptake coefficient (or reaction probability), important in experimental analyses and modeling studies. The relationships between γ_X and $\gamma_{eff,X}$ and related quantities can be efficiently expressed by a gas-phase diffusion correction factor $C_{g,X}$, as previously introduced for gas uptake by spherical particles:[46]

$$C_{g,X} = \frac{\gamma_{eff,X}}{\gamma_X} = \frac{J_{coll,X}}{J_{coll,avg,X}} = \frac{[X]_{gs}}{[X]_g} \quad (7)$$

Mass transport of a gas species to a surface involving molecular diffusion depends on the flow regime. For a flow-tube geometry as illustrated in Figure 1, this is characterized by the Knudsen number, Kn_X, in the form of[70]

$$Kn_X = \frac{2\lambda_X}{D_{tube}} \quad (8)$$

with $\lambda_X = 3D_{g,X}/\omega_X$ as derived by Fuchs and Sutugin.[44]

Typical gas uptake experiments with flow tubes are operated between 1 and 1013 hPa. Under these conditions, the following three flow regimes are possible:

(1) For $Kn_X \gg 1$ and whenever $Kn_X/\gamma_X \gg 1$, termed gas kinetic or free-molecule regime, the flow of X from the gas phase to the wall surface is limited only by surface kinetics and X is homogeneous in the gas phase ($[X]_g = [X]_{gs}$).

(2) For $Kn_X \ll 1$, termed continuum regime, the flow of X is limited only by gas-phase diffusion when $Kn_X/\gamma_X \ll 1$.

(3) For $Kn_X \approx 1$, termed transition regime, when $\gamma_X \approx 1$ and also in the continuum regime when $Kn_X/\gamma_X \approx 1$, the flow of X is influenced by both gas-phase diffusion and uptake. $[X]_g > [X]_{gs}$ for experimental studies whenever $Kn_X/\gamma_X \lesssim 1$ and the relationship between $[X]_g$ and $[X]_{gs}$ is described by $C_{g,X}$ as detailed below.

For the uptake of a gas species X by a cylindrical tube under steady-state conditions, the net flow from the gas phase to the cylinder wall (see Figure 1) can be described by the following gas kinetic expression:

$$F_{net,X} = k_{diff,X}[X]_g V_{tube} \quad (9)$$

where V_{tube} ($= \pi {D_{tube}}^2 z/4$) is the volume enclosed by the wall and $k_{diff,X}$ is the diffusion-limited wall loss rate coefficient, which can be described as

$$k_{diff,X} = 4\frac{N_{Shw}^{eff} D_{g,X}}{{D_{tube}}^2} \quad (10)$$

where N_{Shw}^{eff} is an effective dimensionless mass-transfer coefficient or effective Sherwood number. Under fast flow conditions in a perfectly absorbing tube ($\gamma_X = 1$) at large dimensionless distance ($z^* \gg 0.1$), N_{Shw}^{eff} can be approximated as 3.66.[40,63−65,72−74] At short dimensionless distance, however, the value of N_{Shw}^{eff} can strongly increase,[72] reflecting changes in the radial concentration profile of the entry region, which are particularly relevant for short tubes, small gas diffusivity, and high flow rate. To account for such flow entry effects, we calculated N_{Shw}^{eff} by numerically integrating $N_{Shw}(z^*)$ as given by Davis[72] (Figure 3 of Davis[72]) from 0 to z^*, followed by division through z^*; that is, $N_{Shw}^{eff} = \int_0^{z^*} N_{Shw}(z^*)\, dz^*$. The integration results are very well represented by the following equation describing N_{Shw}^{eff} as a function of z^* (Figure 2):

$$N_{Shw}^{eff} = 3.6568 + A/(z^* + B) \quad (11)$$

with $A = 0.0978$ and $B = 0.0154$.

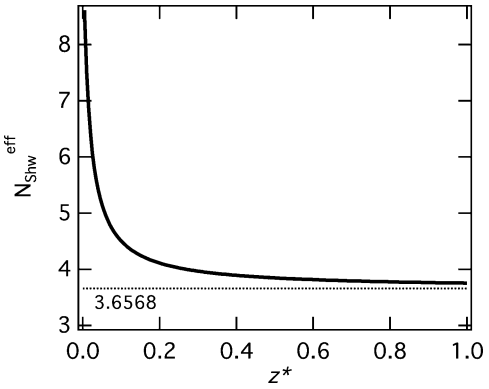

Figure 2. Effective dimensionless mass-transfer coefficient or effective Sherwood number, N_{Shw}^{eff}, calculated as a function of dimensionless tube length, z^* (eq 11).

Combining eqs 9 and 11 results in

$$F_{net,X} = N_{Shw}^{eff}(\pi D_{g,X}) z [X]_g \qquad \text{for } \gamma_X = 1 \quad (12)$$

Following the PRA approach for spherical particles,[46] the net flow of gas-phase diffusion through a virtual tube envelope for an absorbing cylinder can be expressed as

$$F_{net,X} = N_{Shw}^{eff}(\pi D_{g,X}) z([X]_g - [X]_{gs}) \qquad \text{for } \gamma_X \leq 1 \quad (13)$$

The mass balance of $[X]_{gs}$ can be described by use of $J_{net,X}$ and the volume of the near-surface gas phase (V_{gs}; see Figure 1):

$$\frac{d[X]_{gs}}{dt} = \frac{F_{net,X} - J_{net,X} S_{tube}}{V_{gs}} = \frac{N_{Shw}^{eff} D_{g,X}([X]_g - [X]_{gs}) - J_{net,X} D_{tube}}{\lambda_X (D_{tube} - \lambda_X)} \quad (14)$$

where

$$V_{gs} = \frac{\pi {D_{tube}}^2}{4} z - \frac{\pi (D_{tube} - 2\lambda_X)^2}{4} z = \pi \lambda_X z (D_{tube} - \lambda_X)$$

and $S_{tube} = \pi D_{tube} z$. Equation 14 demonstrates the matching of diffusive and net uptake fluxes at a distance λ_X away from the wall surface.

For steady-state conditions, $d[X]_{gs}/dt = 0$ can be inserted in eq 14, and combination with eq 6 followed by rearrangement of the equation leads to the gas-phase diffusion correction factor $C_{g,X}$:

DOI: 10.1021/ac5042395
Anal. Chem. 2015, 87, 3746−3754

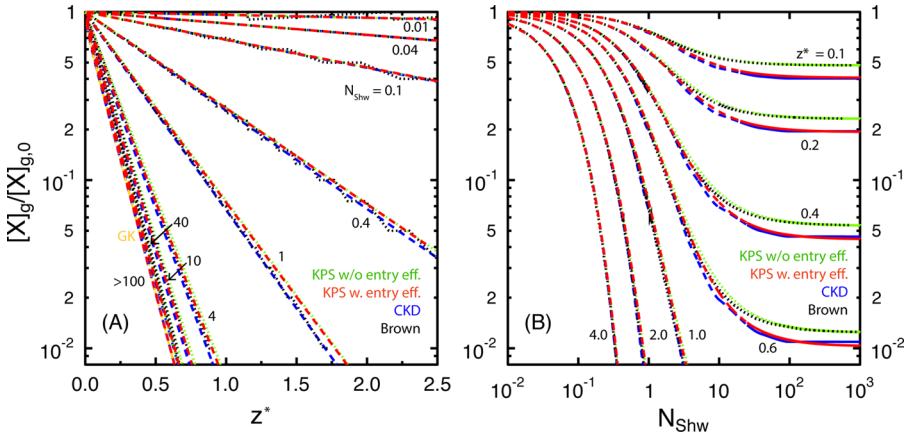

Figure 3. Penetration or tube transmission ($[X]_g/[X]_{g,0}$) for a cylindrical flow reactor, denuder, or sampling tube, calculated (A) as a function of the dimensionless axial distance, z^*, for several values of the Sherwood number N_{Shw} and (B) as a function of N_{Shw} for several z^* values. Different calculation methods are indicated by different line styles: KPS without flow entry effects, green dotted line; KPS with flow entry effects, red dashed line; CKD, blue dashed line; Brown, black dotted line; and GK, yellow dash-dotted line.[61,62]

$$C_{g,X} = \frac{\gamma_{eff,X}}{\gamma_X} = \frac{[X]_{gs}}{[X]_g} = \frac{1}{1 + \gamma_X \frac{\omega_X D_{tube}}{4 N_{Shw}^{eff} D_{g,X}}} = \frac{1}{1 + \gamma_X \frac{3 D_{tube}}{4 N_{Shw}^{eff} \lambda_X}} = \frac{1}{1 + \gamma_X \frac{3}{2 N_{Shw}^{eff} Kn_X}} \quad (15)$$

As outlined by Pöschl et al.,[46] $C_{g,X}$ can also be converted into a gas-phase diffusion conductance term $\Gamma_{g,X}$ for application in traditional resistor model formulations of gas uptake:[75,76]

$$\Gamma_{g,X} = \frac{3}{2 N_{Shw}^{eff} Kn_X} \quad (16)$$

The loss rate of X can be expressed as

$$\frac{d[X]_g}{dt} = -\gamma_{eff,X} J_{coll,avg,X} \frac{S_{tube}}{V_{tube}} = -\gamma_{eff,X} \frac{\omega}{4} [X]_g \frac{\pi D_{tube} z}{\pi/4 D_{tube}^2 z} = -\gamma_{eff,X} \frac{\omega_X}{D_{tube}} [X]_g \quad (17)$$

and the experimentally observable penetration or tube transmission, P_X, is given by

$$P_X = \frac{[X]_g}{[X]_{g,0}} = \exp\left(-\gamma_{eff,X} \frac{\omega_X}{D_{tube}} t\right) \quad (18)$$

where t represents the interaction time between the gas species and the reactive or absorbing wall (with length z) derived from the average laminar flow velocity.

Solving for the net uptake coefficient yields

$$\gamma_{eff,X} = \frac{D_{tube}}{\omega_X t} \ln\left(\frac{[X]_{g,0}}{[X]_g}\right) \quad (19)$$

and eq 15 can be used to derive γ from experimentally determined $\gamma_{eff,X}$ values, that is, to correct the results of kinetic experiments for gas-phase diffusion effects:

$$\gamma_X = \frac{\gamma_{eff,X}}{1 - \gamma_{eff,X} \frac{3}{2 N_{Shw}^{eff} Kn_X}} \quad (20)$$

Combination of eqs 18 and 20 leads to

$$P_X = \frac{[X]_g}{[X]_{g,0}} = \exp\left(-\frac{\gamma_X}{1 + \gamma_X \omega_X D_{tube}/(4 N_{Shw}^{eff} D_{g,X})} \frac{\omega_X}{D_{tube}} t\right) = \exp\left(-\frac{\gamma_X}{1 + 3\gamma_X/(2 N_{Shw}^{eff} Kn_X)} \frac{\omega_X}{D_{tube}} t\right) \quad (21)$$

Equation 21 allows for the prediction of penetration as a function of tube geometry, flow conditions, and uptake coefficient, which reflects the absorptivity or reactivity of the wall surface.

Note that the derivation of the above equations constituting the KPS method does not include the correction term introduced by Motz and Wise[77] to compensate for a distorted velocity distribution at the absorbing wall and has been used in several treatments of gas uptake and diffusion, including the CKD method as given by Murphy and Fahey[55] but not the Brown method.[53] As discussed by Pöschl et al.,[46] the influence of this correction term on the overall effects of gas-phase diffusion and the differences between alternative formulations[43,44] are small and limited to the transition regime. Moreover, the validity of the correction factor of Motz and Wise[77] has recently been disputed by Zhang and Law.[78]

The KPS method provides simple analytical equations to calculate the penetration and correct for the effects of gas-phase diffusion in flow-tube reactors, denuders, or sampling lines. It does not require numerical techniques like the method of Brown[53] or interpolation procedures like the CKD method,[55] which have commonly been applied for analysis or prediction of gas uptake kinetics and wall losses. Below we will show that the KPS method also holds for diffusional losses of particles to a tube wall.

RESULTS AND DISCUSSION

Generic Validation. To validate our new method (KPS), we compare it to the established numerical and interpolation methods of diffusion correction by Brown[53] and CKD.[54,55] To cover a wide range of flow-tube geometries, flow conditions, and uptake kinetics, we calculated the predicted change in penetration or tube transmission, $[X]_g/[X]_{g,0}$, as a function of the dimensionless tube length z^* and the Sherwood number for $\gamma_X \leq 1$, $N_{Shw} = (\omega_X D_{tube}/4D_{g,X})\gamma_X$, as defined by Murphy and Fahey.[55]

DOI: 10.1021/ac5042395
Anal. Chem. 2015, 87, 3746−3754

Figure 3 shows that all methods are in good agreement at $[X]_g/[X]_{g,0} > 0.1$ and $N_{Shw} < 1$, corresponding to low γ_X or low z^*, respectively. At high N_{Shw} and γ_X, the KPS method with flow entry effects (eq 21 with N_{Shw}^{eff} from eq 10) continues to agree with the CKD method, while the KPS method without flow entry effects (eq 21 with $N_{Shw}^{eff} = 3.66$) agrees with the Brown method. Due to enhanced uptake in the flow entry region, the penetration predicted by the CKD method and the KPS method with flow entry effects at $N_{Shw} > 10$ are ~20% lower than the values calculated by the Brown method and the KPS method without flow entry effects (Figure 3B). As discussed by Murphy and Fahey,[55] the penetration predicted by the CKD method is insensitive to the details of wall loss kinetics when N_{Shw} and γ_X are large, approaching the Gormley–Kennedy limit at $N_{Shw} > 100$ and $\gamma_X \approx 1$ (shown as a yellow dash-dotted line in Figure 3A).[61,62] Figure 3B shows that the KPS and Brown methods have higher sensitivity for resolving changes in penetration at very high uptake and $N_{Shw} > 100$, where the slope of the CKD solution drops to zero. For the remainder of this study we will apply only the KPS method with flow entry effects included.

Specific Applications. Having validated the KPS method against established gas-phase diffusion correction methods, we demonstrate its practical applicability by analyzing measurement data from kinetic uptake experiments investigating the reaction of O_3, NO_3, and OH with different organic substrates located on the inside wall of a flow-tube reactor.[23−26,38] These kinetic experiments represent a wide range of multiphase reaction kinetics with γ_X ranging from about 10^{-6} to 0.1, different total pressures, and laminar flow velocities. Table 1 summarizes the experimental conditions of the analyzed kinetic uptake experiments, which were all performed in flow-tube reactors coupled to gas-phase detectors that monitor changes in the average reactant gas-phase concentration $[X]_g$ due to gas uptake on the reactor walls. In the case of OH and NO_3 uptake kinetic studies, a custom-built chemical ionization mass spectrometer (CIMS) was employed to detect changes in $[X]_g$.[24] OH was detected as OH^- following chemical ionization by SF_6^-.[24] NO_3 was detected as NO_3^- by use of I^-.[38] In the ozonolysis experiments, O_3 was detected by a photometric O_3 analyzer.[26] OH radicals were produced by a microwave discharge of H_2 in the presence of O_2.[24] NO_3 radicals were produced by passing the N_2O_5/He gas flow through a Teflon-coated glass oven held at 433 K, inducing thermal dissociation of N_2O_5.[38,79] Ozone was generated by passing a flow of O_2 over an ultraviolet source before it entered the flow-tube reactor.[26]

In each experiment the penetration of the reactant gas was recorded as a function of total exposure time, while the initial gas concentration at the inlet of the flow-tube reactor, $[X]_{g,0}$, as well as the gas–substrate interaction time (t), that is, the contact time between the gas species and the absorbing or reactive wall surface, were kept constant. Figure 4 shows the change in penetration of OH, NO_3, and O_3 measured at the end of the flow-tube reactor. As specified in Table 1, the gas–substrate interaction times differed by orders of magnitude between the different experiments, which thus covered a wide range of uptake kinetics: fast uptake in the OH experiment, intermediate uptake in the NO_3 experiment, and slow uptake in the O_3 experiment. For each set of experimental conditions and measurement data, we applied the Brown, CKD, and KPS methods to characterize the effects of diffusion and derive reactive uptake coefficients.

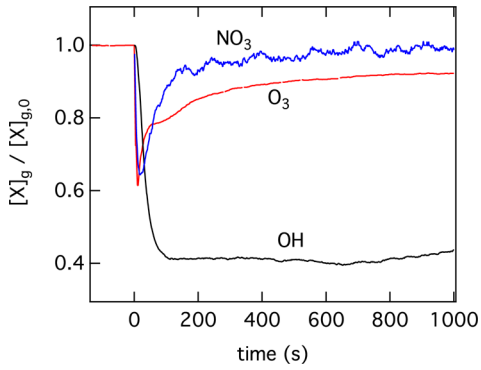

Figure 4. Measured penetration or tube transmittance ($[X]_g/[X]_{g,0}$) plotted as a function of total exposure time for three kinetic experiments in a coated-wall flow-tube reactor: OH uptake by levoglucosan,[24] NO_3 uptake by abietic acid,[25] and O_3 uptake by bovine serum albumin.[26] Experimental conditions are specified in Table 1

Table 1. Summary of Experimental Parameters Applied in Three Different Reactive Uptake Experiments[a]

	OH + levoglucosan[24]	NO_3 + abietic acid[25,38]	O_3 + BSA[26]
T/K	293	298	298
p/hPa	5.3	3.0	1013
Re	22.5	4.2	17.4
Pe	28.71	16.79	190.50
λ/cm	9.35×10^{-3}	9.00×10^{-3}	1.1×10^{-5}
Kn	0.01	0.01	2.8×10^{-5}
$[X_i]_{g,0}$/cm^{-3}	1.71×10^{9}	7.3×10^{10}	2.7×10^{12}
ω/cm·s^{-1}	6.04×10^{4}	3.19×10^{4}	3.6×10^{4}
v/cm·s^{-1}	2874.71	914.45	30.17
D_g/cm^2·s^{-1}	188.22	95.72	0.1267
t/s	0.00126	0.01094	1.657
D_{tube}/cm	1.77	1.758	0.8
l_{tube}/cm	3.6	10	50
z^*	0.15	0.68	0.66

[a]Temperature (T), flow reactor pressure (p), Reynolds number (Re), Peclet number (Pe), mean free path (λ), Knudsen number (Kn), initial gas-phase concentration of species X ($[X]_{g,0}$), thermal molecular velocity (ω), flow velocity (v), diffusion coefficient for given experimental T and p, gas–substrate interaction time (t), tube diameter (D_{tube}), tube length (l_{tube}), and dimensionless axial distance (z^*) are given. BSA, bovine serum albumin.

Figure 5 summarizes the results obtained for the OH uptake experiment. Figure 5A,B shows how the penetration and gas-diffusion correction factor (eqs 21 and 15) depend on the gas uptake coefficient for a dimensionless tube length or axial distance $z^* = 0.15$, which is characteristic for the experimental conditions. Up to $\gamma_X \approx 0.02$, all gas-phase diffusion correction methods predict the same penetration, but at higher γ_X the KPS and CKD methods predict lower penetration than the Brown method, which does not account for flow entry effects. Figure 5C demonstrates that the measurement-derived OH uptake coefficients obtained with the KPS and CKD methods agree within ~10%, whereas the Brown method yields γ_{OH} values that are ~40% higher throughout the duration of the experiment. The OH gas-diffusion correction factors $C_{g,OH}$ displayed in Figure 5D correspond to the ratio of uncorrected to corrected uptake coefficients ($\gamma_{OH,eff}/\gamma_{OH}$) from Figure 5C. In the plot of

DOI: 10.1021/ac5042395
Anal. Chem. 2015, 87, 3746−3754

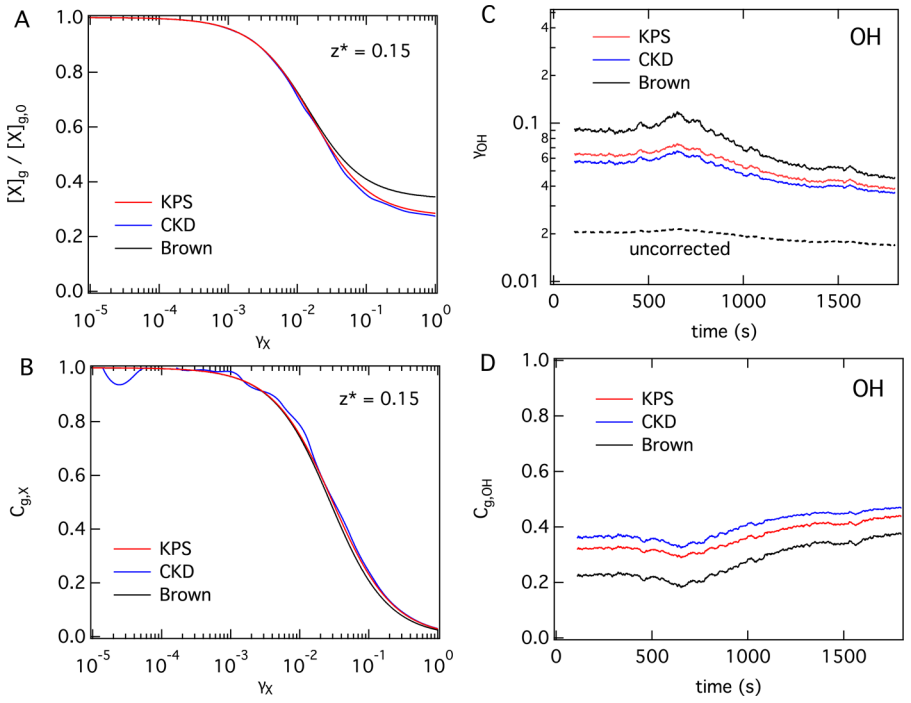

Figure 5. OH uptake experiment analyzed with the KPS (red), CKD (blue), and Brown (black) methods. (A) Penetration and (B) gas-diffusion correction factor as a function of uptake coefficient, calculated for a dimensionless axial distance of $z^* = 0.15$ reflecting the experimental conditions. (C) Measurement-derived uptake coefficient and (D) gas-diffusion correction factor obtained with different diffusion correction methods as a function of exposure time.

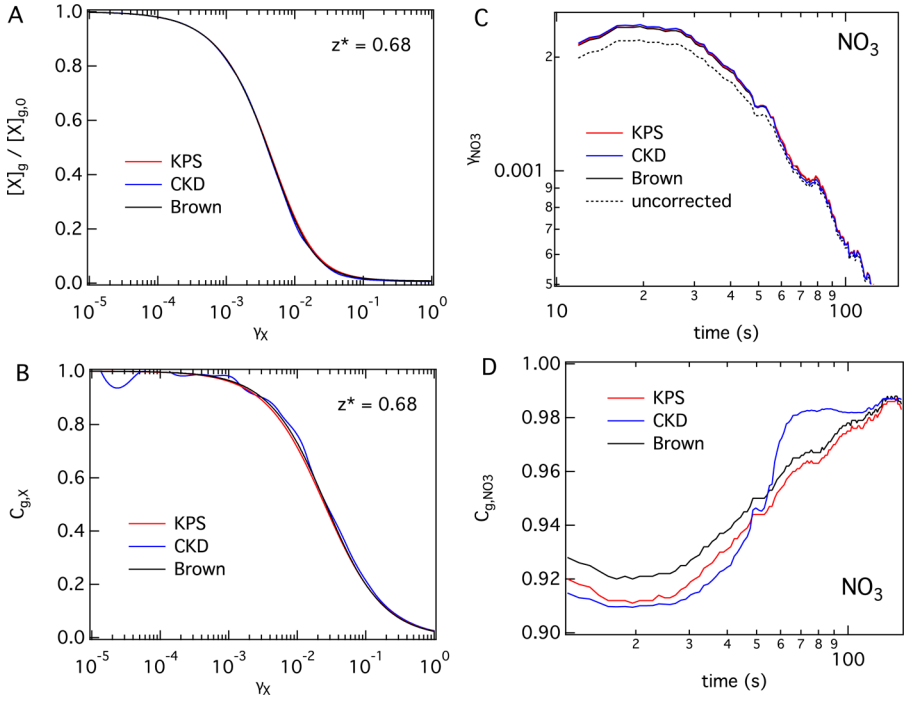

Figure 6. NO_3 uptake experiment analyzed with the KPS (red), CKD (blue), and Brown (black) methods. (A) Penetration and (B) gas-diffusion correction factor as a function of uptake coefficient, calculated for a dimensionless axial distance of $z^* = 0.68$ reflecting the experimental conditions. (C) Measurement-derived uptake coefficient and (D) gas-diffusion correction factor obtained with different diffusion correction methods as a function of exposure time.

$C_{g,X}$ versus γ_X obtained with the CKD method, the small dip around $\gamma_X \approx 2 \times 10^{-5}$ and other minor wiggles are due to numerical artifacts of interpolation. The differences between KPS, CKD, and Brown methods are due to their different treatment of the correction for gas-phase diffusion only and do not include uncertainties in the experimental data or diffusion coefficients.

Figure 6 shows the same analysis as in Figure 5 but for the case of NO_3 uptake by abietic acid substrates. The uptake kinetics are about 2 orders of magnitude slower compared to

DOI: 10.1021/ac5042395
Anal. Chem. 2015, 87, 3746−3754

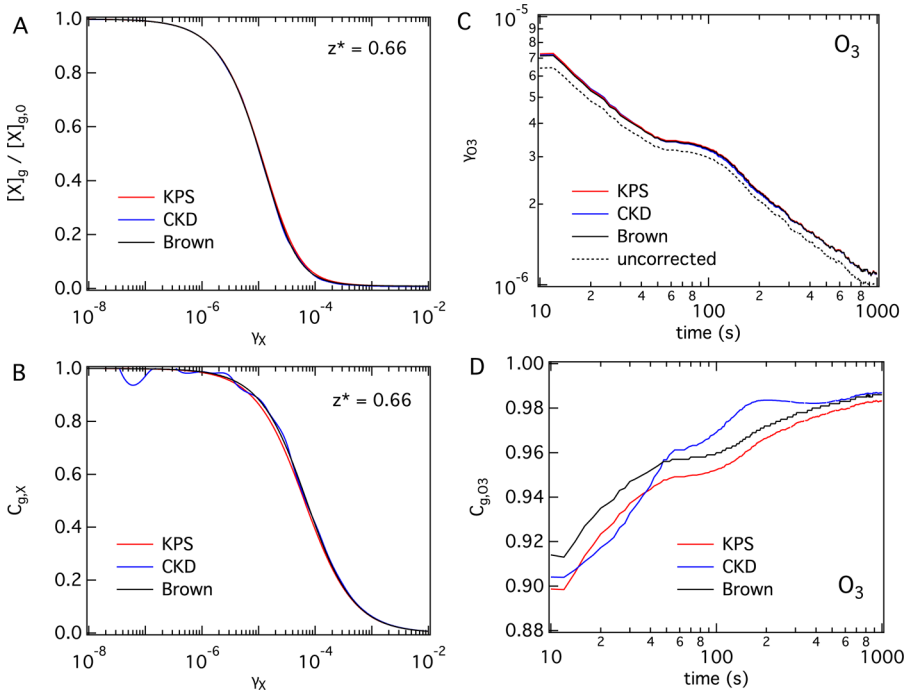

Figure 7. O_3 uptake experiment analyzed with the KPS (red), CKD (blue), and Brown (black) methods. (A) Penetration and (B) gas-diffusion correction factor as a function of uptake coefficient, calculated for a dimensionless axial distance of $z^* = 0.66$ reflecting the experimental conditions. (C) Measurement-derived uptake coefficient and (D) gas-diffusion correction factor obtained with different diffusion correction methods as a function of exposure time.

the OH uptake kinetics discussed above. Figure 6A,B shows the dependence of penetration and gas-diffusion correction factor on the uptake coefficient for the dimensionless axial distance of $z^* = 0.68$, which is characteristic for the NO_3 uptake experiment. All methods agree very well, as flow entry effects are negligible at high z^* (see Figure 2). The correction of γ_{eff,NO_3} is small (~5%) and similar for all applied methods, as demonstrated in Figure 6C. This is further corroborated in Figure 6D by the less than 2% difference between the C_{g,NO_3} values derived by different methods.

Figure 7 displays the analysis results for uptake of O_3 by protein bovine serum albumin (BSA), which exhibits the lowest uptake coefficient of $\gamma_{O_3} < 10^{-5}$. Figure 7A,B displays the dependence of penetration and gas-diffusion correction factor on the uptake coefficient for $z^* = 0.66$, characteristic for the O_3 uptake experiment. As flow entry effects are again not critical under this condition, all methods show very good agreement. The measurement-derived uptake coefficients γ_{O_3} and gas-diffusion correction factor C_{g,O_3} from the different methods agree within 2% (Figure 7C,D).

Diffusion of aerosol particles is treated in the same way as for gas-phase species, namely, by considering the species as spheres.[16,80] In fact, the limiting case of the CKD solution is the GK solution,[55] which is also applied to predict the penetration of an aerosol flow through a tube.[14−16] Therefore, the KPS method should be applicable to diffusion of aerosol particles to the walls of a cylindrical flow tube. Indeed eq 21 can be directly applied for aerosol particles, using particle thermal velocity (ω^p) and diffusion coefficient (D_g^p) corrected by the Cunningham slip correction factor.[80,81] Note that particles exhibit much smaller ω^p and D_g^p values compared to gas species, leading to different Knudsen numbers for otherwise similar experimental conditions. For example, a 1 μm diameter particle with unit density is characterized by $\omega^p = 0.44$ cm·s^{-1} and $D_g^p = 2.7 \times 10^{-7}$ cm^2·s^{-1} at 293 K.[80]

Figure 8 shows the penetration of aerosol particles as a function of the dimensionless deposition parameter μ =

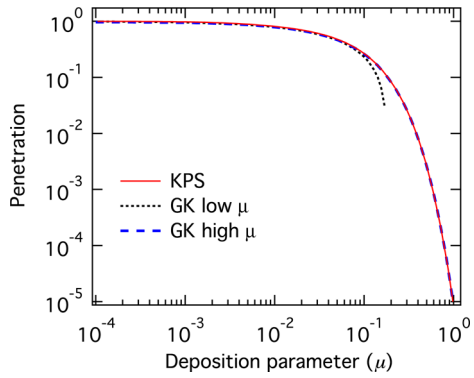

Figure 8. Penetration of aerosol particles in a cylindrical flow tube as a function of deposition parameter μ. Red, blue, and black lines represent the results by the KPS formulation and the two limiting cases of Gormley and Kennedy (GK),[61] respectively.

$D_g^p l_{tube}/Q$ calculated using the GK reference and the KPS method with $\gamma = 1$. Particle losses are small for low μ (corresponding to short tube length, fast flow rate, and/or low diffusivity), whereas nearly all particles are lost to the wall at $\mu \approx 1$ (corresponding to long tube length, slow flow rate, and/or high diffusivity). Two analytical solutions for diffusional loss of particles to a tube wall, as described by Gormley and Kennedy[61] and adapted in the monographs of Hinds[16] and Kulkarni, Baron, and Willeke,[14,15] have been derived and are available for the limiting cases of $\mu \leq 0.02$ and $\mu > 0.02$, which

DOI: 10.1021/ac5042395
Anal. Chem. 2015, 87, 3746−3754

are depicted as the black and blue lines, respectively, in Figure 8. These analytical solutions and KPS agree very well with relative differences ≤2% over the investigated range of μ = 10^{-4}−1.

The KPS line in Figure 8 was calculated for three different particle diameters of 1 μm, 100 nm, and 0.37 nm (diameter of an "air molecule"), which gave indistinguishable results, demonstrating that the treatment of gas and particle diffusion converges in the KPS method.

CONCLUSIONS

A new analytical method has been derived for prediction of the penetration or tube transmission and diffusion of gas molecules and aerosol particles to an absorbing or reactive cylindrical wall of a flow reactor, denuder, or sampling tube. This derivation is based on the recently developed kinetic flux model framework and models that describe the interaction of gas species with aerosol particles[45−49,52] in combination with the well-established diffusion limit of gas and particle uptake by a cylindrical wall.[63,65] A gas-phase diffusion correction factor as well as gas and particle penetration can be calculated from explicit analytical equations, rendering numerical techniques or interpolation methods unnecessary. By analysis of experimental data from OH radical, NO_3 radical, and ozone uptake by aromatic acid, carbohydrate, and protein substrates, we demonstrate that the new KPS method is applicable to rapid, intermediate, and slow uptake conditions. The agreement with more complex numerial and interpolation methods (Cooney−Kim−Davis and Brown) and analytical solutions (Gormley−Kennedy) shows that the KPS method, the underlying flux matching approach, and the PRA framework are generally applicable for interfacial transport, reactions, and losses of gas molecules and aerosol particles. Although derived for gas flow tubes, the analytical equations are general in nature and thus should also hold for other fluid types under laminar flow conditions.

AUTHOR INFORMATION

Corresponding Authors

*(D.A.K.) E-mail daniel.knopf@stonybrook.edu.
*(M.S.) E-mail m.shiraiwa@mpic.de.

Notes

The authors declare no competing financial interest.

ACKNOWLEDGMENTS

We thank D. M. Murphy for helpful discussions and pointing out the importance of flow entry effects. D.A.K. acknowledges support by the National Science Foundation, Grant AGS-0846255. U.P. and M.S. acknowledge funding from the Pan-European Gas−Aerosols−Climate Interaction Study (265148, PEGASOS).

REFERENCES

(1) Howard, C. J. *J. Phys. Chem.* **1979**, *83*, 3−9.
(2) Dryer, F. L.; Haas, F. M.; Santner, J.; Farouk, T. I.; Chaos, M. *Prog. Energy Combust.* **2014**, *44*, 19−39.
(3) McMurry, P. H.; Stolzenburg, M. R. *Atmos. Environ.* **1987**, *21*, 1231−1234.
(4) Hayes, R. E.; Kolaczkowski, S. T.; Thomas, W. J.; Titiloye, J. *Proc. R. Soc. Math. Phys.* **1995**, *448*, 321−334.
(5) Honda, N.; Masuda, A.; Matsumura, H. *J. Non-Cryst. Solids* **2000**, *266*, 100−104.
(6) Alzueta, M. U.; Glarborg, P.; DamJohansen, K. *Combust. Flame* **1997**, *109*, 25−36.
(7) Brown, R. L. *Comput. Chem.* **1984**, *8*, 139−145.
(8) Seeley, J. V.; Jayne, J. T.; Molina, M. J. *J. Phys. Chem.* **1996**, *100*, 4019−4025.
(9) Dasgupta, P. K. *Adv. Chem. Ser.* **1993**, 41−90.
(10) Clemitshaw, K. C. *Crit. Rev. Environ. Sci. Technol.* **2004**, *34*, 1−108.
(11) Kloskowski, A.; Pilarczyk, M.; Namiesnik, J. *Crit. Rev. Anal. Chem.* **2002**, *32*, 301−335.
(12) Spindler, G.; Hesper, J.; Bruggemann, E.; Dubois, R.; Muller, T.; Herrmann, H. *Atmos. Environ.* **2003**, *37*, 2643−2662.
(13) Knopf, D. A.; Zink, P.; Schreiner, J.; Mauersberger, K. *Aerosol Sci. Technol.* **2001**, *35*, 924−928.
(14) Kulkarni, P.; Baron, P. A.; Willeke, K. *Aerosol Measurement: Principles, Techniques, and Applications*, 3rd ed.; John Wiley & Sons: New York, 2011.
(15) Baron, P. A.; Willeke, K. *Aerosol Measurement: Principles, Techniques and Applications*, 2nd ed.; John Wiley & Sons: New York, 2001.
(16) Hinds, W. C. *Aerosol Technology: Properties, Behavior, and Measurement of Airborne Particles*, 2nd ed.; John Wiley & Sons: New York, 1999.
(17) Cussler, E. L. *Diffusion: Mass Transfer in Fluid Systems*; Cambridge University Press: Cambridge, U.K., 2009.
(18) Schmidt, L. D. *Engineering of Chemical Reactions*, 2nd ed.; Oxford University Press: London, 2005.
(19) Fogler, H. S. *Elements of Chemical Reaction Engineering*; Prentice-Hall International: Upper Saddle River, NJ, 2006.
(20) Huang, R. J.; Hoffmann, T. *Anal. Chem.* **2009**, *81*, 1777−1783.
(21) Fisseha, R.; Dommen, J.; Sax, M.; Paulsen, D.; Kalberer, M.; Maurer, R.; Hofler, F.; Weingartner, E.; Baltensperger, U. *Anal. Chem.* **2004**, *76*, 6535−6540.
(22) Eisele, F. L.; Berresheim, H. *Anal. Chem.* **1992**, *64*, 283−288.
(23) Slade, J. H.; Knopf, D. A. *Geophys. Res. Lett.* **2014**, *41*, 5297−5306.
(24) Slade, J. H.; Knopf, D. A. *Phys. Chem. Chem. Phys.* **2013**, *15*, 5898−5915.
(25) Shiraiwa, M.; Pöschl, U.; Knopf, D. A. *Environ. Sci. Technol.* **2012**, *46*, 6630−6636.
(26) Shiraiwa, M.; Ammann, M.; Koop, T.; Pöschl, U. *Proc. Natl. Acad. Sci. U.S.A.* **2011**, *108*, 11003−11008.
(27) Monge, M. E.; D'Anna, B.; Mazri, L.; Giroir-Fendler, A.; Ammann, M.; Donaldson, D. J.; George, C. *Proc. Natl. Acad. Sci. U.S.A.* **2010**, *107*, 6605−6609.
(28) Kolb, C. E.; Cox, R. A.; Abbatt, J. P. D.; Ammann, M.; Davis, E. J.; Donaldson, D. J.; Garrett, B. C.; George, C.; Griffiths, P. T.; Hanson, D. R.; Kulmala, M.; McFiggans, G.; Pöschl, U.; Riipinen, I.; Rossi, M. J.; Rudich, Y.; Wagner, P. E.; Winkler, P. M.; Worsnop, D. R.; O' Dowd, C. D. *Atmos. Chem. Phys.* **2010**, *10*, 10561−10605.
(29) Bartels-Rausch, T.; Huthwelker, T.; Gaggeler, H. W.; Ammann, M. *J. Phys. Chem. A* **2005**, *109*, 4531−4539.
(30) Worsnop, D. R.; Morris, J. W.; Shi, Q.; Davidovits, P.; Kolb, C. E. *Geophys. Res. Lett.* **2002**, *29* (20), 57-1−57-4 DOI: 10.1029/2002GL015542.
(31) Hanson, D. R.; Sugiyama, M.; Morita, A. *J. Phys. Chem. A* **2004**, *108*, 3739−3744.
(32) Longfellow, C. A.; Imamura, T.; Ravishankara, A. R.; Hanson, D. R. *J. Phys. Chem. A* **1998**, *102*, 3323−3332.
(33) Hanson, D. R. *Geophys. Res. Lett.* **1997**, *24*, 1087−1090.
(34) Lambe, A. T.; Ahern, A. T.; Williams, L. R.; Slowik, J. G.; Wong, J. P. S.; Abbatt, J. P. D.; Brune, W. H.; Ng, N. L.; Wright, J. P.; Croasdale, D. R.; Worsnop, D. R.; Davidovits, P.; Onasch, T. B. *Atmos. Meas. Tech.* **2011**, *4*, 445−461.
(35) Zhou, S.; Shiraiwa, M.; McWhinney, R. D.; Pöschl, U.; Abbatt, J. P. D. *Faraday Discuss.* **2013**, *165*, 391−406.
(36) Ammann, M.; Cox, R. A.; Crowley, J. N.; Jenkin, M. E.; Mellouki, A.; Rossi, M. J.; Troe, J.; Wallington, T. J. *Atmos. Chem. Phys.* **2013**, *13*, 8045−8228.

DOI: 10.1021/ac5042395
Anal. Chem. 2015, 87, 3746−3754

(37) Crowley, J. N.; Ammann, M.; Cox, R. A.; Hynes, R. G.; Jenkin, M. E.; Mellouki, A.; Rossi, M. J.; Troe, J.; Wallington, T. J. *Atmos. Chem. Phys.* **2010**, *10*, 9059−9223.
(38) Knopf, D. A.; Forrester, S. M.; Slade, J. H. *Phys. Chem. Chem. Phys.* **2011**, *13*, 21050−21062.
(39) Knopf, D. A.; Anthony, L. M.; Bertram, A. K. *J. Phys. Chem. A* **2005**, *109*, 5579−5589.
(40) Danckwerts, P. V. *Ind. Eng. Chem.* **1951**, *43*, 1460−1467.
(41) Danckwerts, P. V. *Trans. Faraday Soc.* **1951**, *47*, 1014−1023.
(42) Danckwerts, P. V. *Trans. Faraday Soc.* **1950**, *46*, 300−304.
(43) Fuchs, N. A. *Mechanics of Aerosols*; Pergamon: New York, 1964.
(44) Fuchs, N. A.; Sutugin, A. G. In *Topics in Current Aerosol Research*; Hidy, G. M., Brock, J. R., Eds.; Pergamon: New York, 1971.
(45) Ammann, M.; Pöschl, U. *Atmos. Chem. Phys.* **2007**, *7*, 6025−6045.
(46) Pöschl, U.; Rudich, Y.; Ammann, M. *Atmos. Chem. Phys.* **2007**, *7*, 5989−6023.
(47) Shiraiwa, M.; Pfrang, C.; Koop, T.; Pöschl, U. *Atmos. Chem. Phys.* **2012**, *12*, 2777−2794.
(48) Pfrang, C.; Shiraiwa, M.; Pöschl, U. *Atmos. Chem. Phys.* **2010**, *10*, 4537−4557.
(49) Shiraiwa, M.; Garland, R. M.; Pöschl, U. *Atmos. Chem. Phys.* **2009**, *9*, 9571−9586.
(50) Kaiser, J. C.; Riemer, N.; Knopf, D. A. *Atmos. Chem. Phys.* **2011**, *11*, 4505−4520.
(51) Springmann, M.; Knopf, D. A.; Riemer, N. *Atmos. Chem. Phys.* **2009**, *9*, 7461−7479.
(52) Shiraiwa, M.; Pfrang, C.; Pöschl, U. *Atmos. Chem. Phys.* **2010**, *10*, 3673−3691.
(53) Brown, R. L. *J. Res. Natl. Bur. Stand.* **1978**, *83*, 1−8.
(54) Cooney, D. O.; Kim, S. S.; Davis, E. J. *Chem. Eng. Sci.* **1974**, *29*, 1731−1738.
(55) Murphy, D. M.; Fahey, D. W. *Anal. Chem.* **1987**, *59*, 2753−2759.
(56) Walker, R. E. *Phys. Fluids* **1961**, *4*, 1211−1216.
(57) Sideman, S.; Luss, D.; Peck, R. E. *Appl. Sci. Res.* **1964**, *14*, 157−171.
(58) Davis, H. R.; Parkinso, G. V. *Appl. Sci. Res.* **1970**, *22*, 20−30.
(59) Tan, C. W.; Hsu, C. J. *J. Aerosol Sci.* **1971**, *2*, 117−124.
(60) Lekhtmakher, S. O. *J. Eng. Phys.* **1971**, *20*, 400−402.
(61) Gormley, P. G.; Kennedy, M. *Proc. R. Ir. Acad., Sect. A* **1949**, *52A*, 163−169.
(62) Bowen, B. D.; Levine, S.; Epstein, N. *J. Colloid Interface Sci.* **1976**, *54*, 375−390.
(63) Ferguson, E. E.; Fehsenfeld, F. E.; Schmeltekopf, A. L. In *Advances in Atomic and Molecular Physics*; Bates, D. R., Ed.; Academic Press, Inc.: New York, 1969.
(64) Gershenzon, Y. M.; Grigorieva, V. M.; Ivanov, A. V.; Remorov, R. G. *Faraday Discuss.* **1995**, 83−100.
(65) Zasypkin, A. Y.; Grigor'eva, V. M.; Korchak, V. N.; Gershenson, Y. M. *Kinet. Catal.* **1997**, *38*, 772−781.
(66) Langmuir, I. *J. Am. Chem. Soc.* **1916**, *38*, 2221−2295.
(67) Hinshelwood, C. N. *The Kinetics of Chemical Change*; Clarendon: Oxford, U.K., 1940.
(68) Eley, D. D.; Rideal, E. K. *Proc. R. Soc. London, Ser. A* **1941**, *178*, 0429−0451.
(69) Rideal, E. K. *Proc. R. Soc. London, Ser. A* **1939**, *35*, 130−132.
(70) Wutz, M.; Adam, H.; Walcher, W. *Theory and Practice of Vacuum Technology*; Friedrich Vieweg & Sohn: Braunschweig/Wiesbaden, Germany, 1989.
(71) Bird, R. B.; Stewart, W. E.; Lightfoot, E. N. *Transport Phenomena*; John Wiley & Sons: New York, 2007.
(72) Davis, E. J. *J. Phys. Chem. A* **2008**, *112*, 1922−1932.
(73) Pöschl, U.; Canagaratna, M.; Jayne, J. T.; Molina, L. T.; Worsnop, D. R.; Kolb, C. E.; Molina, M. J. *J. Phys. Chem. A* **1998**, *102*, 10082−10089.
(74) Jayne, J. T.; Pöschl, U.; Chen, Y. M.; Dai, D.; Molina, L. T.; Worsnop, D. R.; Kolb, C. E.; Molina, M. J. *J. Phys. Chem. A* **1997**, *101*, 10000−10011.
(75) Kolb, C. E.; Worsnop, D. R.; Zahniser, M. S.; Davidovits, P.; Keyser, L. F.; Leu, M.-T.; Molina, M. J.; Hanson, D. R.; Ravishankara, A. R.; Williams, L. R.; Tolbert, M. A. In *Progress and Problems in Atmospheric Chemistry*; Barker, J. R., Ed.; World Scientific: Singapore, 1995; pp 771−875.
(76) Schwartz, S. E. In *Chemistry of Multiphase Atmospheric Systems*; Jaeschke, W., Ed.; Springer: New York, 1986.
(77) Motz, H.; Wise, H. *J. Chem. Phys.* **1960**, *32*, 1893−1894.
(78) Zhang, P.; Law, C. K. *J. Fluid Mech.* **2009**, *634*, 113−135.
(79) Knopf, D. A.; Mak, J.; Gross, S.; Bertram, A. K. *Geophys. Res. Lett.* **2006**, *33*, No. L17816.
(80) Seinfeld, J. H.; Pandis, S. N. *Atmospheric Chemistry and Physics: From Air Pollution to Climate Change*; John Wiley: New York, 1998; p 1326.
(81) Cunningham, E. *Proc. R. Soc. London, Ser. A* **1910**, *83*, 357−365.

DOI: 10.1021/ac5042395
Anal. Chem. 2015, 87, 3746−3754